Rare Metal Materials and Engineering
Volume 50, Issue 11, November 2021
Available online at www.rmme.ac.cn

Science Press

Cite this article as: Wang Yixuan, Jia Lina, Zhang Hu. Influence of Temperature Gradient on Microstructure and Microhardness of Directionally Solidified Al-Zn-Mg-Cu Alloy[J]. Rare Metal Materials and Engineering, 2021, 50(11): 3910-3916.

ARTICLE

Influence of Temperature Gradient on Microstructure and Microhardness of Directionally Solidified Al-Zn-Mg-Cu Alloy

Wang Yixuan, Jia Lina, Zhang Hu

Department of Materials Science and Engineering, Beihang University, Beijing 100191, China

Abstract: The Al-Zn-Mg-Cu alloy with high Zn content was cast at different temperature gradients by directional solidification. The primary dendrite arm spacing λ_1, the secondary dendrite arm spacing λ_2, and the Vickers hardness of specimens were characterized. Based on the experiment results, the relationship among temperature gradient, dendritic arm spacing, and microhardness was determined by linear regression analysis and curve fitting analysis. The results are in agreement with the dendritic growth theoretical models, and the solidification parameters of Al-Zn-Mg-Cu alloy were obtained. In addition, the influence mechanism of temperature gradient on microhardness was analyzed. The results have a guidance function on the optimization of preparing methods of Al-Zn-Mg-Cu alloy with high zinc content.

Key words: Al-Zn-Mg-Cu alloys; directional solidification; temperature gradient; dendrite arm spacing; theoretical model

The age-hardening Al-Zn-Mg-Cu aluminum alloys (AA7XXX series) are widely used for aircraft structures and various critical military facilities due to their excellent combinations of high strength and lightweight[1-3]. The strength of AA7XXX series alloys can be obviously improved with increasing the Zn content[4-6]. However, when Zn content is more than 8wt%, the phenomenon of grain coarsening and serious macrosegregation occurs more likely. Moreover, due to the large temperature difference between liquid phase and solid phase during the solidification of Al-Zn-Mg-Cu aluminum alloys, the non-equilibrium solidified eutectic structures can be formed at the grain boundary. Therefore, hot cracking easily occurs in the casting, leading to poor casting performance and negative effect on the subsequent extrusion process[7], which seriously restricts the application of Al-Zn-Mg-Cu aluminum alloys in industry.

To predict and control the solidification structure and to improve the properties of as-cast Al-Zn-Mg-Cu aluminum alloys, the formation mechanism of dendrite spacing and its relationship with the solidification conditions, especially the temperature gradient during cooling, should be investigated. However, since solidification is a complex process involving heat, mass, and momentum transfer, numerous experiments and theoretical studies on dendrite spacing were conducted using directionally solidified single-phase alloys, such as Al-Cu, Al-Mg, and Al-Fe alloys[8-17]. In addition, complete models of the relationship among solidification condition, microstructure, and mechanical properties were established. But similar models for solidified multi-phase alloys, such as Al-Zn-Mg-Cu alloys, were barely reported. In recent years, Xie[18] and Yan[19] et al studied the microstructure and microsegregation of solidified 7050Al alloy by directional solidification and modified the Scheil model, but the relationship between solidification condition and mechanical properties was still imprecise.

In this research, the relationship among primary dendrite arm spacing (λ_1), secondary dendrite arm spacing (λ_2), microhardness, and the temperature gradient (G, particularly the one caused by specimen diameter) of Al-8.9Zn-2.1Mg-1.8Cu-0.13Zr aluminum alloy was obtained and the related models were established. Moreover, the effect of temperature gradient on microhardness and related mechanism were discussed. The results provide more information for the solidification process of Al-Zn-Mg-Cu aluminum alloys.

Received date: November 09, 2020
Foundation item: National Key R&D Program of China (2016YFB0300900)
Corresponding author: Jia Lina, Ph. D., Professor, Department of Materials Science and Engineering, Beihang University, Beijing 100191, P. R. China, Tel: 0086-10-82316482, E-mail: jialina@buaa.edu.cn

1 Experiment

The Al-Zn-Mg-Cu material used in this research was Al-8.9Zn-2.1Mg-1.8Cu-0.13Zr alloy ingot, and its chemical composition is presented in Table 1. In order to obtain different temperature gradients, Al_2O_3 tubes of high purity with inner diameter of 4, 7, 12, and 15 mm and length of 200 mm were used to load the specimens with different diameters for the directional solidification. The directional solidification of specimens was performed in the Bridgman-type directional solidification furnace using liquid Ga-In-Sn as the cooling medium, as shown in Fig.1. The specimens were superheated to 750 °C for 1 h before directional solidification, and then solidified at a drawing velocity of 100 μm/s. The solidified specimens were subsequently cut along longitudinal and transverse directions for further observation.

The longitudinal and transverse sections of the specimens were inlaid in bakelite powder at 130 °C. The specimens were then ground with 240#~3000# SiC paper, polished with diamond pastes of 0.5 μm, and etched by Keller's reagent (1.5 mL HCl, 1 mL HF, 2.5 mL HNO_3, and 95 mL H_2O) for 25 s. Because the secondary dendrite arms of specimens could not be observed clearly after corrosion by Keller's reagent, Weck's reagent (100 mL H_2O, 4 g $KMnO_4$, 1 g NaOH) was used to corrode the longitudinal section to measure the secondary dendrite arm spacing. The specimens were observed by Carl Zeiss optical microscope (OM). The dendritic arm spacings (λ_1 and λ_2) were measured using the Image J software, and the magnification factor was taken into consideration.

The values of λ_1 on the transverse sections were measured using the triangle method[20]. The triangle was formed by joining three neighbor dendrite centers, and the length of the triangle sides was referred as λ_{1T}, as shown in Fig. 2. On the longitudinal section, the primary dendrite arm spacing along longitudinal direction λ_{1L} was obtained by measuring the distance between the nearest two dendrites tips. During the measurements, the values of λ_{1T} and λ_{1L} were measured 50~80 times for each specimen. The λ_1 value used in analysis was the average value of λ_{1T} and λ_{1L}.

Table 1 Composition of Al-Zn-Mg-Cu alloy (wt%)

Zn	Mg	Cu	Zr	Fe	Si	Al
8.9	2.1	1.8	0.13	≤0.15	≤0.15	Bal.

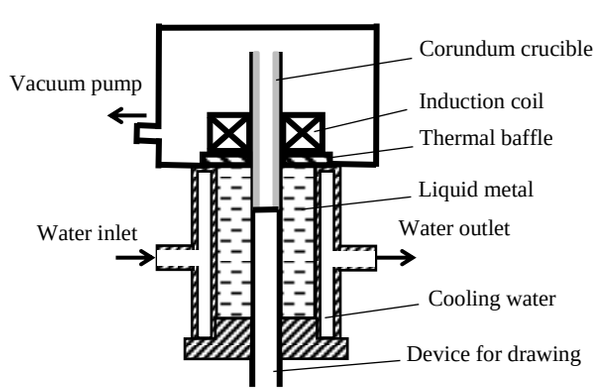

Fig.1 Schematic diagram of Bridgman-type directional solidification furnace

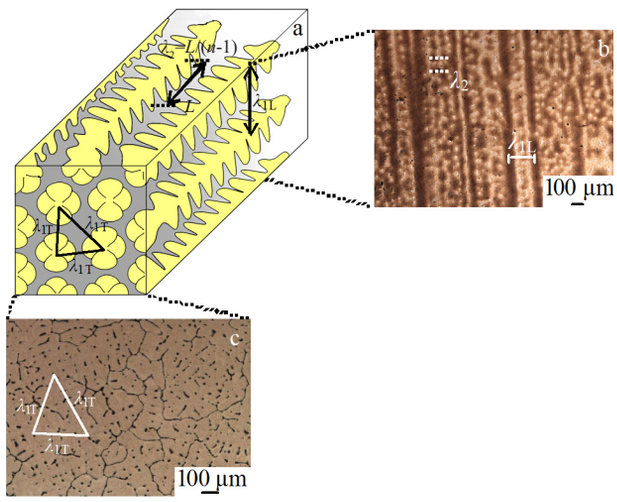

Fig.2 Schematic diagrams of dendritic arm spacing measurement: (a) longitudinal and transverse sections; (b) measurement of λ_{1L} and λ_2 on longitudinal section; (c) measurement of λ_{1T} by triangle method and area counting method on transverse section

The values of λ_2 were measured by averaging the distances between adjacent side branches on the longitudinal section of primary dendrites, as shown in Fig. 2. All the secondary dendrite arm spacing data used in this research were the average value of the initial λ_2 value of 25~40 primary dendrites in each specimen.

Microhardness was measured by a micro-Vickers sclerometer under a load of 200 g and a dwell time of 10 s. The microhardness was measured at least twenty times on transverse and longitudinal sections of each specimen. Due to the composition segregation, inhomogeneities in the microstructure, and error in judging indentation boundary, some errors were unavoidable. In order to reduce the error, the maximum and minimum values were removed and then the average of remaining values was calculated and used.

According to the heat balance equation of directional solidification and assuming that the radial heat flow in the melt is neglected, the temperature gradient of liquid phase (G_L) at the liquid-solid interface can be obtained as follows[12,21]:

$$G_L = \frac{1}{K_L}(K_S G_S - \rho L_f v) = \frac{1}{K_L}\left[\frac{2h\alpha(T - T_0)}{vr} - \rho L_f v\right] \quad (1)$$

where K_L and K_S are the thermal conductivity of the liquid and solid phases, respectively; G_S is the temperature gradient of solid phase; ρ is density of the alloy; L_f is latent heat of crystallization; v is drawing velocity; h is the composite heat transfer coefficient between the casting and the cooling

medium; α is thermal diffusivity; T is the casting temperature; T_0 is the temperature of the cooling medium; r is radius of the specimen.

Some parameter values calculated by JMatPro software are shown in Table 2. The temperature at which the alloy begins to solidify is substituted by the casting temperature T. The room temperature is taken as the temperature of cooling medium T_0.

For composite heat transfer coefficient h, the heat transfer coefficient of conduction, convection, and radiation can be set as h_c, h_f, h_R, respectively. Then h can be obtained by Eq.(2) as follows:

$$h=h_c+h_f+h_R \quad (2)$$

Since the specimen was directly inserted into the cooling medium during the directional solidification, h_R in the fluid is 0 and the thermal resistance between the specimen and the Al_2O_3 tube is very small. Then Eq. (3) can be obtained, as follows:

$$h\approx h_f \quad (3)$$

When Ga-In-Sn liquid metal was used as cooling medium[22,23], Eq.(3) can be transformed as Eq.(4), as follows:

$$h\approx h_f=14\ 122\ \mathrm{W/m^2\cdot K} \quad (4)$$

The results of calculated temperature gradient are shown in Table 3.

Table 2 Parameters used in experiment

Parameter	Value
Casting temperature, T/K	903
Cooling medium temperature, T_0/K	298
Thermal conductivity of liquid phase, K_L/W·m^{-1}·K^{-1}	86.73
Latent heat of crystallization, L_f/J·g^{-1}	4.1
Thermal diffusivity, α/m^2·s^{-1}	2.95×10^{-9}
Drawing velocity, v/μm·s^{-1}	100
Alloy density, ρ/g·cm^{-3}	2.55

2 Results and Discussion

2.1 Effect of temperature gradient on dendritic arm spacings

Fig. 3 and Fig. 4 show the OM images of longitudinal and transverse sections of Al-Zn-Mg-Cu alloys after directional solidification at the steady-state conditions under different temperature gradients with a constant growth rate of V=100 μm/s.

For the calculation of primary dendrite arm spacing λ_1, Hunt[23] firstly established the function of solidification parameters (V, G, C_0). Assuming that the front dendrite can be regarded as a sphere, which is determined by the minimum undercooling, the Hunt model can be expressed by Eq.(5) as follows:

$$\lambda_1 = 2.83\left[m(k-1)D\Gamma\right]^{0.25}C_0^{0.25}V^{-0.25}G^{-0.5} \quad (5)$$

where m is liquidus slope, k is partition coefficient, D is diffusion coefficient in liquid, Γ is the Gibbs-Thomson coefficient, and C_0 is the initial concentration of solute.

Trivedi[24] modified the Hunt model by introducing marginal stability criterion, and λ_1 was obtained as follows:

$$\lambda_1 = 2.83\left[m(k-1)D\Gamma L\right]^{0.25}C_0^{0.25}V^{-0.25}G^{-0.5} \quad (6)$$

where L is a constant depending on harmonic perturbation.

The theoretical model developed by Kurz et al[25] assumed that the shape of the dendrite can be regarded as ellipsoid, and used the marginal stability criterion for the isolated dendrite.

Table 3 Temperature gradients G of different specimens

Specimen diameter/mm	G/K·mm^{-1}
4	2.91
7	1.66
12	0.97
15	0.77

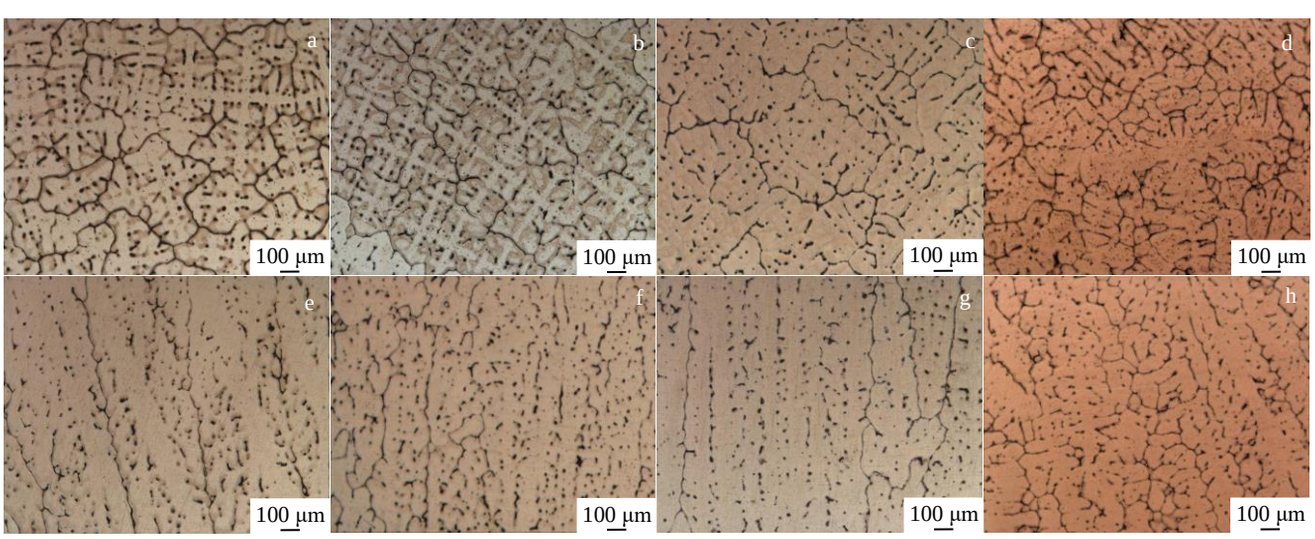

Fig.3 OM images of transverse (a~d) and longitudinal (e~h) sections of directionally solidified Al-Zn-Mg-Cu alloys with different diameters etched in Keller's reagent: (a, e) 4 mm, (b, f) 7 mm, (c, g) 12 mm, and (d, h) 15 mm

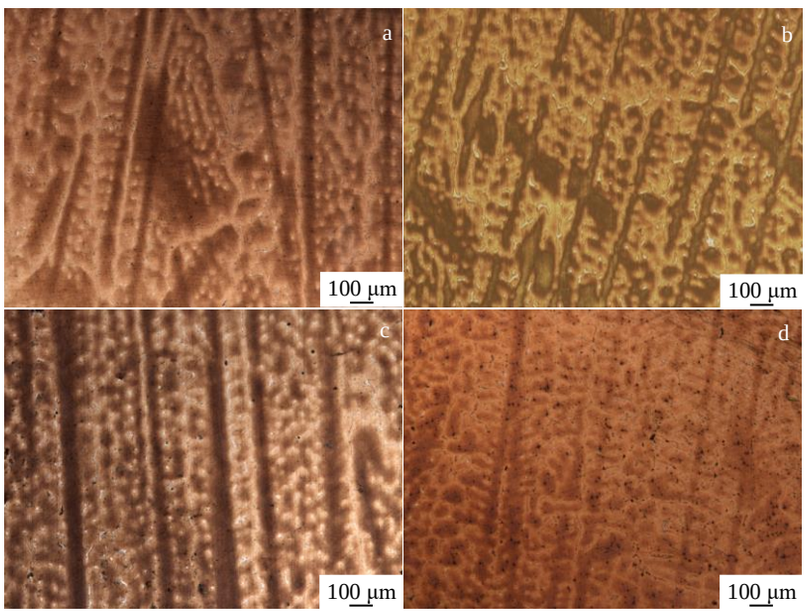

Fig.4 OM images of longitudinal sections of directionally solidified Al-Zn-Mg-Cu alloy with different diameters etched in Weck's reagent: (a) 4 mm, (b) 7 mm, (c) 12 mm, and (d) 15 mm

Then the model can be expressed by Eq.(7) as follows:

$$\lambda_1 = 4.3\left[m(k-1)D\Gamma/k^2\right]^{0.25} C_0^{0.25} V^{-0.25} G^{-0.5} \quad (7)$$

When the parameters except temperature gradient are fixed, all the models based on single-valued selection can be simplified as Eq. (8), indicating that λ_1 is a function of temperature gradient G, which can be expressed as follows:

$$\lambda_1 = k_1 G^{-0.5} \quad (8)$$

In semi-analytic computation, the relationship between λ_2 and the local solidification time τ_f is generally used to describe the secondary dendrite arm coarsening process, which ultimately leads to the equation between λ_2 and τ_f or the cooling rate c_R[8,26]:

$$\lambda_2 = Bc_R^{-l} \quad (9)$$

$$\lambda_2 = M\tau_f^p \quad (10)$$

where the coefficients M and B are related to the alloy composition; the local solidification time $\tau_f=(T_L-T_S)/VG$ (T_L is the liquidus temperature and T_S is the solidus temperature); the exponent p is equal to 1/3 in general, depending on the chosen coarsening model; the exponent l is obtained from experiment.

For the exponent p in Eq.(10), it does not always remain at 1/3, and can be affected by other factors such as the liquidus and the distribution coefficient. The exponent p is increased with increasing the slope of the liquidus, and decreased with increasing the distribution coefficient[27]. Then the model can be simplified as follows:

$$\lambda_2 = k_2 G^{-p} \quad (11)$$

The relationship between microstructure parameters (λ_{1L}, λ_{1T}, and λ_2) and temperature gradient was determined by a curve fitting analysis. The fitting results are shown in Table 4. As shown in Table 4 and Fig.5, with increasing the temperature gradient, the dendrite arm spacings (λ_1, λ_2) are decreased.

Table 4 Relationships between microstructure parameters and temperature gradient

Dendrite arm spacing	Relationship	Square of correlation coefficient, R^2
λ_1	$\lambda_{1T}=193G^{-0.51}$	0.99
	$\lambda_{1L}=204G^{-0.41}$	0.93
	$\lambda_1=199G^{-0.45}$	0.97
λ_2	$\lambda_2=57G^{-0.18}$	0.90

The relationships between microstructure parameters (λ_1, λ_2) and the diameter of specimen are $\lambda_{1T}=193G^{-0.51}$, $\lambda_{1L}=204G^{-0.41}$, $\lambda_1=199G^{-0.45}$, and $\lambda_2=57G^{-0.18}$. The experiment data are reasonably in agreement with the derived formulas.

According to the reports about the relationships between the temperature gradient and microstructures (λ_1, λ_2) in previous works[8,10-16], it can be seen that even if the experiment is conducted under similar conditions (similar composition of specimen, drawing rate, or temperature gradient), the results vary and are distributed in dispersion. Besides, the results can be influenced not only by the drawing rate, temperature gradient, or the specimen composition, but also by the anisotropy of the solid-liquid interfacial energy, molecular attachment kinetics[28], convections[29,30], change of growth direction[31], impurities, ripening process, and heating and cooling rate on the specimen. Compared with the results in this research, the relationship between λ_1 and temperature gradient is in agreement with that in previous works[8,10-16]. Though there are some differences in relationship between λ_2 and temperature gradient, it still conforms to the exponential function.

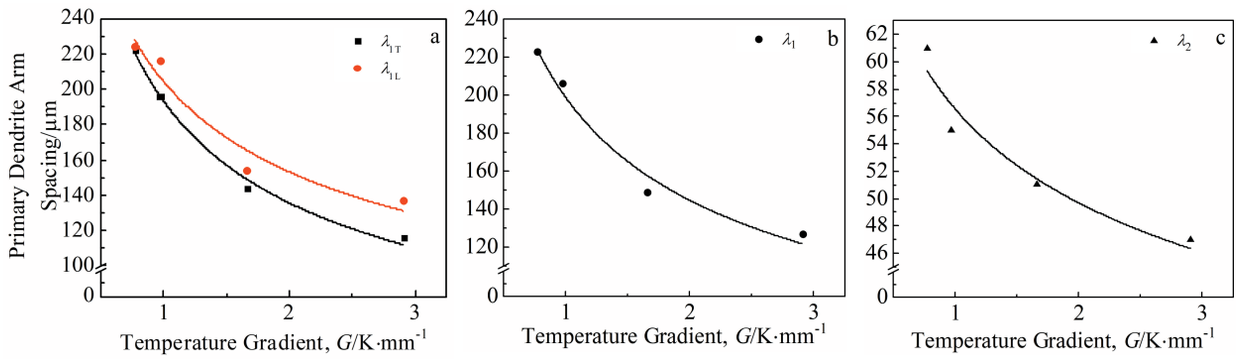

Fig.5 Relationship between dendrite arm spacing of $\lambda_{1T}/\lambda_{1L}$ (a), λ_1 (b), and λ_2 (c) and temperature gradient G at constant drawing velocity of 100 μm/s

2.2 Effect of dendritic arm spacings on microhardness

The Hall-Petch type equation[32,33] describes the relationship between yield strength σ or microhardness HV and grain size of a polycrystalline material, indicating that grain refinement is an effective way to improve the mechanical properties of polycrystalline materials in the conventional grain size range of micrometer. Hence, the relationship between microhardness and the grain size can be described as follows:

$$HV = HV_0 + k_3 d^{-0.5} \quad (12)$$

where HV_0 is the initial microhardness of equilibrated phase; d is the average grain diameter; k_3 is a constant depending on materials. Xie et al[18] replaced the grain size with the primary dendrite arm spacing λ_1 and the secondary dendrite arm spacing λ_2. Then the equation can be expressed as follows:

$$HV = HV_0 + k_4 \lambda_1^{-0.5} \quad (13)$$

$$HV = HV_0 + k_5 \lambda_2^{-0.5} \quad (14)$$

where k_4 and k_5 are constants depending on materials. HV_0, k_4, and k_5 can be determined by experiments.

Based on the previous analysis, the relationship between microhardness and λ_{1L}, λ_{1T}, and λ_2 was determined by a linear regression analysis. As shown in Table 5 and Fig. 6, with increasing the dendrite arm spacings (λ_1, λ_2), the microhardness is decreased. The fitting results are in agreement with the inferences deduced from Hall-Petch type equation, namely, Eq. (13) and Eq. (14). Therefore, increasing the temperature gradient results in finer dendritic microstructures, thereby increasing the microhardness HV. The relationships between microhardness HV, microhardness along transverse direction HV_T, microhardness along longitudinal direction HV_L and dendrite arm spacing λ_{1L}, λ_{1T}, λ_1, and λ_2 are $HV_T = 69+733\lambda_{1T}^{-0.5}$, $HV_L = 53+1050\lambda_{1L}^{-0.5}$, $HV = 61+883\lambda_1^{-0.5}$, and $HV = -36+1201\lambda_2^{-0.5}$.

Table 5 Relationships between microhardness and microstructure parameters

Dendrite arm spacing	Relationship	Pearson correlation coefficient, r
λ_1	$HV_T = 69+733\lambda_{1T}^{-0.5}$	0.97
	$HV_L = 53+1050\lambda_{1L}^{-0.5}$	0.99
	$HV = 61+883\lambda_1^{-0.5}$	0.97
λ_2	$HV = -36+1201\lambda_2^{-0.5}$	0.99

2.3 Effect of temperature gradient on microhardness

The Hall-Petch relation is derived from the dislocation stacking model[24,25]. Due to different orientations of atomic arrangement of adjacent grains and sub-grains on both sides of grain boundary, the grain boundary is in a distorted state. The dislocation density at grain boundary is large, which hinders the metal slip and dislocation movement, and therefore the grain boundary strengthening occurs. In addition, as for the as-

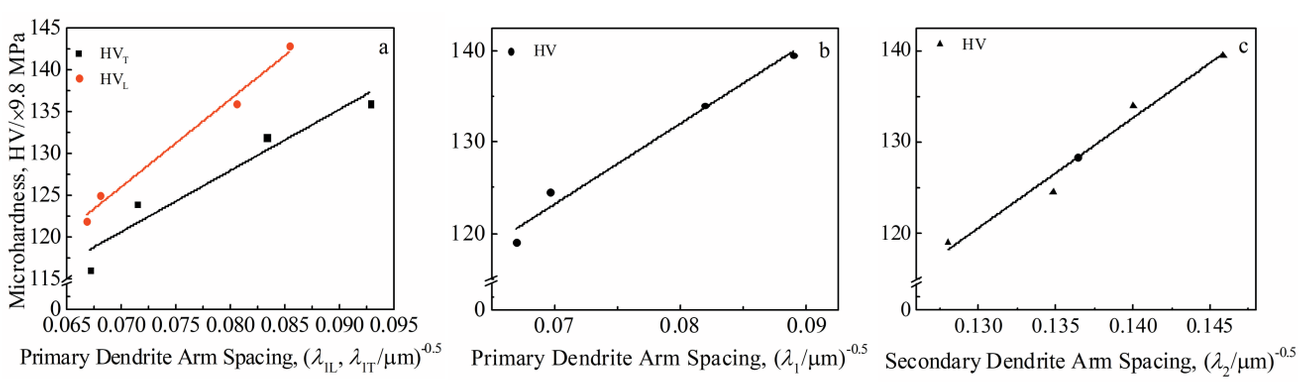

Fig.6 Relationship between microhardness and dendritic arm spacing of $\lambda_{1T}/\lambda_{1L}$ (a), λ_1 (b), and λ_2 (c) at constant drawing velocity of 100 μm/s

cast Al-Zn-Mg-Cu aluminum alloy, the hard precipitation phase at the grain boundary also contributes to improving the microhardness of the alloy. The crystal structure of the second phase particles is different from that of the matrix. When the dislocation breaks through the particles, it will inevitably cause the mismatch of atomic arrangement on the slip surface, thus increasing the slip resistance.

According to the relationships in Table 4 and Table 5, the relationships between temperature gradient and microhardness can be directly obtained, as listed in Table 6. After directional solidification, the transverse grain boundary which is perpendicular to the temperature gradient direction of the alloy is mainly eliminated. In microhardness measurement, the probability of indenter pressing on dendrites with the same orientation in longitudinal section is higher than that in cross section. The effect of grain boundary strengthening on the longitudinal section is weaker than that on the cross section. However, the effect of primary dendrite arm spacing in the longitudinal section on the temperature gradient is slightly stronger than that in the cross section, as shown in Fig. 7, which proves that the second phase strengthening makes a major contribution to the improvement of microhardness of the alloy. The Hall-Petch relationship can still fit well because the second phase of as-cast Al-Zn-Mg-Cu alloy is concentrated at grain boundary. Three relationships between the primary dendrite arm spacing and microhardness are close to each other, while the relationship between the secondary dendrite spacing and microhardness is quite different. This may be because the second phase between the secondary dendrites is mostly spherical with dispersive distribution, which has little effect on the microhardness.

Table 6 Relationships between temperature gradient and microhardness

Dendrite arm spacing	Relationship
λ_1	$HV_T=69+52.76G^{0.255}$
	$HV_L=53+73.51G^{0.205}$
	$HV=61+59.05G^{0.225}$
λ_2	$HV=-36+159.08G^{0.09}$

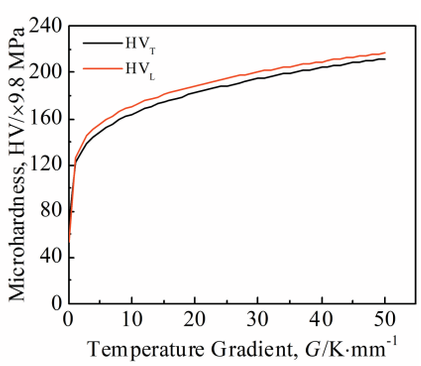

Fig.7 Relationship between microhardness and temperature gradient at constant drawing velocity of 100 μm/s

The diffusion time of elements in dendrites is decreased with increasing the temperature gradient, which causes serious segregation and the fact that more continuous non-equilibrium solidification phases with network structure are formed at the grain boundary. The relation between HV and G can be obtained by synthesizing the above relationships: $HV=61+59.05G^{0.225}$. When the temperature gradient increases, the grain size becomes smaller, but the non-equilibrium phase between grain boundaries is increased. The presence of continuous non-equilibrium solidification phase between grain boundaries enhances the microhardness, but it also becomes the origin of defects. If the solidification phase is too much, it will not be easily eliminated by subsequent homogenization treatment, thus affecting the quality of extruded products. According to the relationship in Table 6, controlling the appropriate temperature gradient and avoiding excessive non-equilibrium solidification phase on the premise of forming finer grains are beneficial to the improvement of properties of as-cast Al-Zn-Mg-Cu aluminum alloy.

3 Conclusions

1) The values of primary dendrite arm spacing λ_1 and the secondary dendrite arm spacing λ_2 are decreased with increasing the temperature gradient G. The relationships between microstructure parameters (primary dendrite arm spacing along transverse direction λ_{1T}, primary dendrite arm spacing along longitudinal direction λ_{1L}, λ_1, λ_2) and the diameter of specimen are $\lambda_{1T}=193G^{-0.51}$, $\lambda_{1L}=204G^{-0.41}$, $\lambda_1=199G^{-0.45}$, and $\lambda_2=57G^{-0.18}$.

2) Increasing the temperature gradient results in finer dendritic microstructures, thereby increasing the microhardness HV. The relationships between microhardness HV (microhardness along transverse direction HV_T, microhardness along longitudinal direction HV_L, HV) and λ_{1L}, λ_{1T}, λ_1, and λ_2 are $HV_T=69+733\lambda_{1T}^{-0.5}$, $HV_L=53+1050\lambda_{1L}^{-0.5}$, $HV=61+883\lambda_1^{-0.5}$, and $HV=-36+1201\lambda_2^{-0.5}$. The fitting results are in good agreement with the Hall-Petch type equation.

3) The relation between HV and G can be obtained by synthesizing the above relationships: $HV=61+59.05G^{0.225}$. When the temperature gradient increases, the grain size becomes smaller, but the non-equilibrium phase between grain boundaries is increased, which easily becomes the crack origin. According to the relationship, selecting a proper temperature gradient can optimize the properties of as-cast Al-Zn-Mg-Cu aluminum alloy.

References

1 Williams J C, Starke Jr E A. *Acta Materialia*[J], 2003, 51(19): 5775

2 Heinz A, Haszler A, Keidel C *et al*. *Materials Science & Engineering A*[J], 2000, 280(1): 102

3 Dursun T, Soutis C. *Materials & Design*[J], 2014, 56: 862

4 Li Xuezhao. *Microstructure and Metallography of Aluminum*

Alloy Materials[M]. Beijing: Metallurgical Industry Press, 2010 (in Chinese)
5 Chen Songyi, Li Jiyu, Hu Guiyun *et al*. *Journal of Alloys and Compounds*[J], 2018, 757: 259
6 Shu W X, Hou L G, Zhang C *et al*. *Materials Science & Engineering A*[J], 2016, 657: 269
7 Guo H M, Yang X J, Wang J X *et al*. *Transactions of Nonferrous Metals Society of China*[J], 2010, 20(3): 355
8 Young K P, Kerkwood D H. *Metallurgical Transactions A*[J], 1975, 6(1): 197
9 Acer E, Çadırlı E, Erol H *et al*. *Metallurgical and Materials Transactions A*[J], 2016, 47(6): 3040
10 An Geying, Liu Lixin. *Journal of Crystal Growth*[J], 1987, 80(2): 383
11 McCartney D G, Hunt J D. *Acta Metallurgica*[J], 1981, 29(11): 1851
12 Gündüz M, Çadırlı E. *Materials Science and Engineering A*[J], 2002, 327(2): 167
13 Su R J, Overfelt R A, Jemian W A. *Metallurgical and Materials Transactions A*[J], 1998, 29(9): 2375
14 Cadirli E, Gündüz M. *Journal of Materials Science*[J], 2000, 35(15): 3837
15 Liu Y L, Kang S B. *Materials Science and Technology*[J], 1997, 13(4): 331
16 Liang D, Jie W, Jones H. *Journal of Crystal Growth*[J], 1994, 135(3-4): 561
17 Sharp R M, Hellawell A. *Journal of Crystal Growth*[J], 1969, 5(3): 155
18 Xie Fanyou, Yan Xinyan, Ding Ling *et al*. *Materials Science & Engineering A*[J], 2003, 355(1-2): 144
19 Yan Xinyan, Ding Ling, Chen Shuanglin *et al*. *130th TMS Annual Meeting*[C]. New Orleans: Springer, 2016: 512
20 Ganesan S, Chan C L, Poirier D R. *Materials Science & Engineering A*[J], 1992, 151(1): 97
21 Qu Min, Liu Lin, Tang Fengtao *et al*. *The Chinese Journal of Nonferrous Metals*[J], 2008, 18(2): 282 (in Chinese)
22 Luo Ruiying, Wang Xianhui, Shi Zhengxing *et al*. *Hot Working Technology*[J], 1995, 24(4): 49 (in Chinese)
23 Hunt J D. *Solidification and Casting of Metals*[M]. London: The Metal Society, 1979
24 Trivedi R. *Metallurgical & Materials Transactions A*[J], 1984, 15(6): 977
25 Kurz W, Fisher D J. *Acta Metallurgica*[J], 1981, 29(1): 11
26 Won Y M, Thomas B G. *Metallurgical and Materials Transactions A*[J], 2001, 32(7): 1755
27 Ode M, Kim S G, Kim W T *et al*. *ISIJ International*[J], 2001, 41(4): 345
28 Glicksman M E, Schaefer R J, Ayers J D. *Metallurgical Transactions A*[J], 1976, 7(11): 1747
29 Hu Xiaowu, Li Shuangming, Gao Sifeng *et al*. *Transactions of Nonferrous Metals Society of China*[J], 2011, 21(1): 65
30 Yu L, Ding G L, Reye J *et al*. *Metallurgical and Materials Transactions A*[J], 2000, 31(9): 2275
31 Henry S, Minghetti T, Rappaz M. *Acta Materialia*[J], 1998, 46(18): 6431
32 Hall E O. *Proceedings of the Physical Society: Section B*[J], 1951, 64(9): 747
33 Petch N J. *Journal of the Iron and Steel Institute*[J], 1953, 174: 25

温度梯度对定向凝固 Al-Zn-Mg-Cu 合金微观组织和硬度的影响

王熠璇，贾丽娜，张　虎
(北京航空航天大学 材料科学与工程学院，北京 100191)

摘　要：采用定向凝固方法制备不同温度梯度下的高锌 Al-Zn-Mg-Cu 合金，表征了该合金的一次枝晶臂间距λ_1、二次枝晶臂间距λ_2以及其维氏硬度。在此基础上，采用线性回归和曲线拟合分析方法建立了温度梯度、枝晶间距和显微硬度之间的关系，结果与枝晶生长理论模型吻合，并获得了高锌 Al-Zn-Mg-Cu 合金的凝固特征参数，同时分析了温度梯度对显微硬度的影响机制。研究结果对高锌 Al-Zn-Mg-Cu 合金制备工艺优化有指导作用。

关键词：Al-Zn-Mg-Cu 合金；定向凝固；温度梯度；枝晶臂间距；理论模型

作者简介：王熠璇，女，1995 年生，硕士生，北京航空航天大学材料科学与工程学院，北京 100191，电话：010-82316482，E-mail：yixuan_wang@buaa.edu.cn